



OPEN ACCESS

EDITED BY

Mariasavina Severino,
Giannina Gaslini Institute (IRCCS), Italy

REVIEWED BY

Efterpi Pavlidou,
University of Ioannina, Greece
Ana Filipa Geraldo,
Centro Hospitalar de Vila Nova de Gaia,
Portugal

*CORRESPONDENCE

Andrea D. Praticò

✉ andrea.pratico@unict.it
Martino Ruggieri

✉ m.ruggieri@unict.it

SPECIALTY SECTION

This article was submitted to Pediatric
Neurology, a section of the journal Frontiers in
Pediatrics

RECEIVED 17 November 2022

ACCEPTED 28 February 2023

PUBLISHED 30 March 2023

CITATION

Praticò AD, Falsaperla R, Comella M, Belfiore G,
Polizzi A and Ruggieri M (2023) Case report: A
gain-of-function of hamartin may lead to a
distinct “inverse *TSC1*-hamartin” phenotype
characterized by reduced cell growth.
Front. Pediatr. 11:1101026.
doi: 10.3389/fped.2023.1101026

COPYRIGHT

© 2023 Praticò, Falsaperla, Comella, Belfiore,
Polizzi and Ruggieri. This is an open-access
article distributed under the terms of the
[Creative Commons Attribution License \(CC BY\)](https://creativecommons.org/licenses/by/4.0/).
The use, distribution or reproduction in other
forums is permitted, provided the original
author(s) and the copyright owner(s) are
credited and that the original publication in this
journal is cited, in accordance with accepted
academic practice. No use, distribution or
reproduction is permitted which does not
comply with these terms.

Case report: A gain-of-function of hamartin may lead to a distinct “inverse *TSC1*-hamartin” phenotype characterized by reduced cell growth

Andrea D. Praticò^{1*}, Raffaele Falsaperla², Mattia Comella¹,
Giuseppe Belfiore³, Agata Polizzi⁴ and Martino Ruggieri^{1*}

¹Unit of Clinical Paediatrics, Department of Clinical and Experimental Medicine, University of Catania, Catania, Italy, ²Units of Neonatology and Neonatal Intensive Care and Paediatrics and Paediatric Emergency, Azienda Ospedaliero Universitaria “Policlinico”, Catania, Italy, ³Unit of Paediatric Radiology, Department of Radiodiagnostics, Azienda Ospedaliero Universitaria “Policlinico”, Catania, Italy, ⁴Chair of Paediatrics, Department of Educational Sciences, University of Catania, Catania, Italy

Mutations of *TSC1* and *TSC2* genes cause classical Tuberous Sclerosis Complex (TSC), a neurocutaneous disorder characterized by a tendency to develop hamartias, hamartomas, and other tumors. We herein report on a girl, now aged 5 years, who presented a previously unreported, distinct clinical phenotype consisting of primary microcephaly (head circumference = 40 cm, −5.6 standard deviations), brain anomalies including hypoplasia of the corpus callosum (with a residual draft of the genu), simplified parieto-temporal gyral pattern, colpocephaly with ectasia of the temporal ventricular horns, intellectual disability, and a general pattern of reduced growth (with weight and height < 3rd centiles). No classical features of TSC were recorded; the girl harbored a novel missense variant in *TSC1* (c.611G>A). We hypothesize that her clinical phenotype could be related to a “gain-of-function” of the *TSC1* protein product hamartin, causing an increase in the effects of the protein on inhibition of its intracellular targets (i.e., mTORC or RAC1 pathways), resulting in a distinct “inverse *TSC1*-hamartin” phenotype characterized by reduced growth of cells instead of the more classical predisposition to increased cell growth.

KEYWORDS

TSC1, hamartin, tuberous sclerosis complex, microcephaly, brain cortical malformations

Introduction

Mutations in *TSC1* and *TSC2* genes lead to abnormal production of hamartin and tuberin, two powerful suppressors of the mTOR pathway of cellular growth, causing the well-known Tuberous Sclerosis Complex (TSC) phenotype [MIM # 191100 and # 613254] (1–3). TSC is characterized by multi-organ involvement including multiple hypomelanotic macules, facial (e.g., forehead plaque), truncal (e.g., shagreen patches) and ungual fibromas, facial angiofibromas, dental enamel pits, multiple cardiac rhabdomyomas, angiomyolipomas and cysts of the kidney and lungs (and other organs), bone dysplasia and overgrowth, brain cortical tubers, subependymal nodules, linear white matter anomalies and subependymal giant cell astrocytoma, epilepsy, psychomotor delay/intellectual disability, and behavioral abnormalities with increased risk of manifesting autism spectrum disorders. Clinically, the range of involvement and phenotype severity is

wide, even within families: affected persons may present only a few skin manifestations with null to minimal neurological involvement or a severe multi-organ and neurodevelopmental disorder with psychomotor delay, drug-resistant seizures, autism, and a predisposition to develop brain and other organ tumors.

The two proteins involved in the pathogenesis of TSC (i.e., *TSC1*/hamartin and *TSC2*/tuberin) cause a single disease, as their action is targeted, in “cooperation”, towards the same cellular pathway, primarily the mechanistic target of rapamycin complex 1 (mTORC1), and other complex inhibitory intracellular mediators or pathways of cellular growth and migration (e.g., RAC1 and RHO G-protein pathways). A direct genotype-phenotype correlation has been established in many studies, but sometimes a single gene variant has been linked to different phenotypes, thus suggesting that other genes or environmental/intracellular factors can contribute to the overall clinical phenotype (4–6). All the mutations and gene variants causing TSC have been shown to be “loss-of-function” mutations, causing impaired, reduced, or absent activity of one of the two proteins. Haploinsufficiency is another important aspect to consider, in that both *TSC1* and *TSC2* are expressed in an autosomal dominant fashion and a single mutation of a single copy is sufficient to cause the clinical phenotype.

To the best of our knowledge, no “hyperactivating” [i.e., gain-of-function] mutations of *TSC1* or *TSC2* have been reported to date in individuals with TSC; other diseases caused by mutation of genes involved in the synthesis of downstream effectors of *TSC1* and *TSC2* have been reported in recent years, including a neurocutaneous phenotype caused by RHOA inactivation and other clinical entities due to Rac1 inactivation, which present with under- or over-growth of the brain depending on the residual function of the protein involved (7–10).

We report on a girl presenting a disease-causing mutation of *TSC1* without stigmata of TSC, but with great similarity to the Rac1-related syndrome (i.e., a complex brain malformation syndrome, including severe primary microcephaly, simplified gyration pattern and other corpus callosum, and ventricle abnormalities). To explain, pathogenically, this phenotype, we hereby hypothesize a gain-of-function effect of the *TSC1* gene variant on hamartin and increased, rather than decreased, inhibition of the mTOR and/or Rac1 pathways, thus leading to the definition of a distinct (likely novel) phenotype with reduced brain cellular growth.

Case report

The proband, a girl, is the only child of healthy, non-consanguineous parents. She was first referred to our Unit of Clinical Pediatrics at the age of 18 months for a diagnostic workup regarding her microcephaly. She was born at 39 weeks of gestation by caesarean section; the pregnancy was characterized by an ultrasonography diagnosis of microcephaly, reduced gyral pattern, and agenesis of the corpus callosum at gestational age 25 weeks. Serological screening for congenital infections (i.e., Cytomegalovirus, *Toxoplasma gondii*, Varicella-Zoster Virus, and

Hepatitis C Virus) during pregnancy and at birth (in the mother and her daughter) was negative, as was the proband neonatal extensive screening for inborn errors of metabolism. Her birth weight was 2.6 kg, height was 47 cm, and head circumference was 32 cm (all below the 3rd percentile). Neonatal history was negative, and she was not breast-fed by the mother.

At our first diagnostic workup, at age 18 months, her weight was 8.4 kg (<3rd percentile), height was 74 cm (<3rd percentile), and head circumference was 38.5 cm (<3rd percentile, –5.6 standard deviations). Three small hyperpigmented maculae (1-cm diameter each) were present on her abdomen. The mother reported irritability and sleep disorders (insomnia). She underwent a new heart examination by means of ECG and echocardiography, abdominal ultrasound, and full ophthalmological examination, all of which were normal. Her eye-to-eye and social interaction with parents and other people was within normal limits, but she was not able to walk alone and spoke only a few words. Brain MRI and additional laboratory and instrumental investigations were planned but the family was temporarily lost to follow-up due to the Covid-19 pandemic.

At the age of 3.5 years, the family again referred the child for completion of her diagnostic work-up. At that stage, brain MRI showed microcephaly with a small brain, simplified parieto-temporal gyral pattern, hypoplasia of the corpus callosum, with a residual draft of the genu, and enlargement and flattening of the ventricles, with colpocephaly and ectasia of the temporal horns (Figure 1). At the age of 4 years, her general conditions were good. Her weight and height were 12.1 kg and 89 cm, respectively (<3rd percentile), head circumference was 40 cm (<3rd percentile, –5.6 standard deviations), the girl was able to walk, did not present any seizures, and showed moderate intellectual disability [IQ by means of WPPSI-III = 67; verbal comprehension index = 61; visual spatial index = 72; fluid reasoning index = 63; working memory index = 70; processing speed index = 69]. She was assisted by a support teacher at school and was under speech-language therapy twice a week.

The girl and her parents underwent next-generation sequencing (NGS) testing with a panel of 161 genes related to brain malformations. A novel variant (c.611G > A), in one copy of the *TSC1* gene, was found in the child, and not in her parents (interpreted as a *de novo* variant). An in-silico analysis was performed using VarCards, ProAffiMuSeq, and Mutation Taster tools (11–15) (see the following sections). Over the following months, the variant was confirmed by Sanger sequencing of the gene; the girl and her parents were also submitted to a further whole exome sequencing analysis, which confirmed the results of the NGS panel and failed to find additional variants in other genes. The *TSC1* variant was hypothesized to cause a gain-of-function effect on hamartin, and consequent hyperactivation of its downstream effectors.

Genetic analysis

The gene panel for brain malformations consisted of 161 genes sequenced by NextSeq 500 System Sequencing [Table 1].

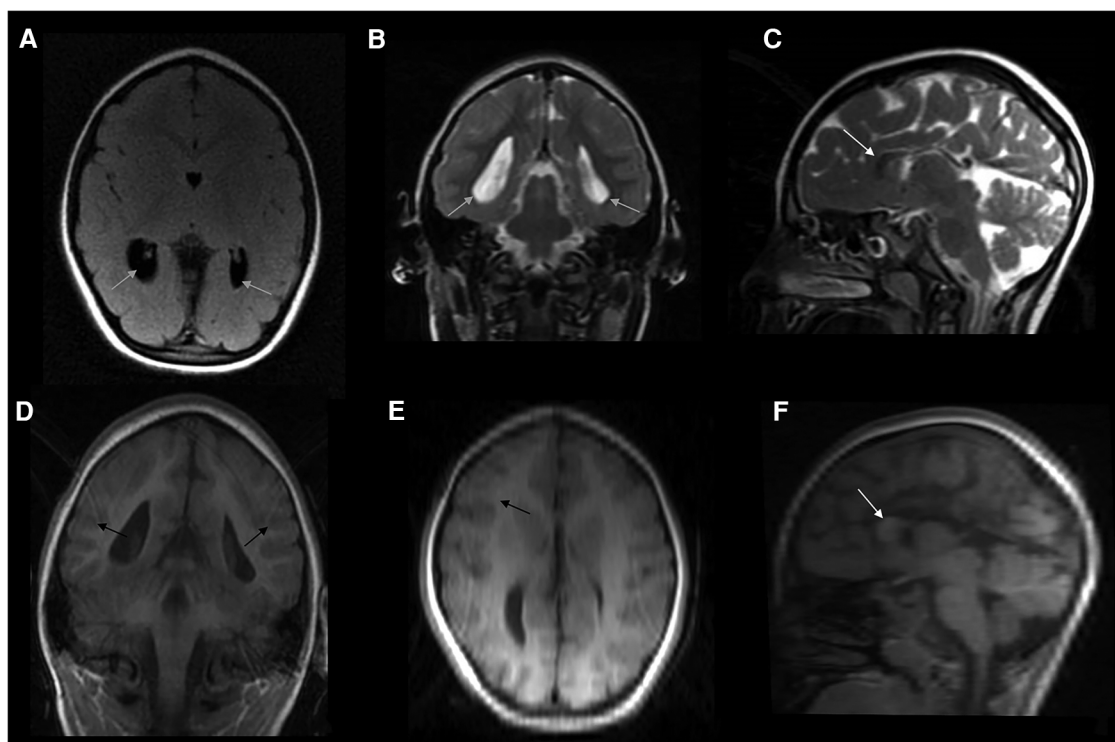


FIGURE 1

Composite panel of six neuroimages showing the brain MRI study in the girl, at the age of 3.5 years: FLAIR-axial scan (A), T2-weighted coronal (B), and sagittal (C) sections; and coronal T1 3D scan (D), as well as reconstructions (reformat) derived from this last study both in axial (E) and sagittal (F) planes. A complex picture of microcephaly, partial agenesis of the corpus callosum with remnants of the genu (white arrow), simplified gyral pattern especially in the parietal and occipital regions of both hemispheres; enlarged and flattened ventricles (grey arrows), with colpocephaly and ectasia of temporal horns were also present. Apparently, no changes in myelin composition and cortical thickness were noticed (black arrows), even if the image protocol shown in this figure is of low quality due to partial panel reformatting. No signs or stigmata of TSC were detected within the brain (e.g., cortical tubers).

Sequencing was preceded by selective enrichment of the regions of the DNA analyzed, through hybridization with selectively designed probes (Sureselect, Agilent). The average coverage of the target bases was <math><100\times</math>.

The resulting variants were therefore analyzed using the BWA software (V.0.7.7-r441), Picard (v 1.109), and GATK (v 3.1), and annotation was performed using Annovar (v. 17June15). All the non-synonymous exonic variants and splice sites (± 2 nucleotides of the coding exons) with frequencies lower than 0.1% for dominant genes and lower than 1% for recessive genes (ExAC, GnomAD) were considered in the analysis. Data obtained through NGS sequencing were therefore analyzed with the tool CoNVaDING in order to identify variants of copy number of the exons (14) and variants reported within the Human Genetic Mutation Database (HGMD) nomenclature. The novel variant (c.611G>A) found in one copy of the *TSC1* gene was found in the proband and not in her parents.

In-silico analysis of the *TSC1* gene variant

The *TSC1* variant c.611G>A recorded herein is associated with replacement of an arginine residue with histidine (both

amino acids harbor “basic” side chains) in position 204 of the protein hamartin (R204H). The change occurs in exon 8, within the “rho-activating domain” (aa 145–510) of hamartin, close to the tuberlin-binding site (aa 302–430). No other variants were found in the remaining genes.

This R204H amino acid substitution was analyzed using different in silico-tools.

Its effects on *hamartin* function were predicted as deleterious by 22/23 tools in the **VarCards** prediction software [which analyses the effects of a gene variant in a set of 23 tools], with an overall damage score of 0.96 [range 0–1].

Such results, however, do not provide accurate information on potential *gain, loss, or changes of function*, thus the “mutated” protein was further tested using the **ProAffiMuSeq** tool (11, 13), a webserver that calculates the binding free energy change ($\Delta\Delta G$ in kcal/mol) for mutant protein-to-protein complexes. Using this tool, we analyzed the *affinity* of the “mutated” hamartin to tuberlin (enzyme complex with non-inhibitor models) and to Rho-GTPase Rac1 (protein-inhibitor model) by comparing the recorded variant and substitution at position 204 to two known variants and substitutions occurring at position 204, which are related to classical TSC phenotypes (R204C and R204P). In all these three genetic “models” (R204P, R204C, and R204H) the affinity of hamartin to Rac1 was decreased, with substantial

TABLE 1 A list of the 161 genes included in the NGS panel for brain malformations searched in our patient.

Gene	Gene	Gene	Gene
ACTB	CSPPI	MCPHI	SEPSSECS
ACTG1	CUL4B	MFSD2A	SHH
ADGRG1	DAG1	MKS1	SIX3
AHI1	DCHS1	MTOR	SLC25A19
AKT1	DCX	MYCN	STAMPB
AKT3	DEPDCS	NDE1	STIL
AMPD2	DYNC1H1	NEDD4L	STRADA
ANKLE2	EML1	NFIX	TBC1D20
ARFGEF2	EMX2	NPHP1	TBC1D7
ARL13B	ERMARD	NPRL2	TBCD
ARX	EXOSC3	NPRL3	TCTN1
ASNS	EXOSC8	NSD1	TCTN2
ASPM	EZH2	OCLN	TCTN3
ATRX	FAT4	OFD1	TGIF1
B3GALNTZ	FIG4	OPHN1	TMEM138
B4GAT1	FKRP	ORC1	TMEM216
B9D1	EKTN	PAFAH1B1	TMEM231
C5orf42	FLNA	PCLO	TMEM237
CASK	FOXC1	PDE6D	TMEMS
CC2D1A	GLI2	PHC1	TMEM67
CC2D2A	GMPPB	PI4KA	TMTC3
CCND2	GNAQ	PIK3CA	TSC1
CDK5	GPSM2	PIK3R2	TSC2
CDK5RAP2	IER3IP1	PLK4	TSEN15
CDK6	INPPSE	POMGNT1	TSEN2
CDON	ISPD	POMGNT2	TSEN34
CENPE	KANSL1	POMT1	TSEN54
CENPJ	KAT6A	POMT2	TUBA1A
CEP135	KATNB1	PPP1R15B	TUBA8
CEP152	KIAA0556	PQBP1	TUBB
CEP290	KIAA0586	PTCH1	TUBB2A
CEP41	KIF11	PTEN	TUBB2B
CEP63	KIF2A	RAB18	TUBB3
CHMP1A	KIF5C	RAB3GAP1	TUBG1
CIT	KIF7	RAB3GAP2	VLDLR
CLP1	KNL1	RARS2	VPS53
CNTNAP2	LAMA2	RELN	VRK1
COL4A1	LAMB1	RPGRIP1L	WDR62
COL4A2	LAMC3	RTTN	YWHAE
CRADD	LARGE1	SASS6	ZIC1
			ZNF423

differences in terms of $\Delta\Delta G$ (4.49, 2.03, and 0.54, respectively). The interaction with tuberlin gave contrasting results: R204P and R204H showed increased affinity ($\Delta\Delta G$ was -0.21 and -0.04 , respectively), while R204C showed decreased affinity ($\Delta\Delta G$ 1.39) [Table 2].

The three tested genetic variants/substitutions (R204P, R204C, and R204H) were further analyzed using **Mutation Taster**, which compares the predicted “amino acid change” score: this latter change is taken from an amino acid substitution matrix (Grantham Matrix) (12), which takes into account the physical-chemical features of amino acids and scores substitutions according to the degree of difference between the original and the new amino acid. Scores may range from 0.0 to 215. The variant/substitution detected herein (i.e., R204H) had a score of 29 (mild effect on hamartin function), while the two other mutations had scores that were 3 to 6 times higher [Table 2].

Discussion

TSC1 and *TSC2* loss-of-function mutations/variants lead to impaired function of the hamartin/tuberlin complex (which is a dimer) and in turn to the classical TSC phenotype. The increased oncological risk of TSC has been explained by the reduced inhibition of the mTOR pathway, which is a very strong activator of protein synthesis and cell growth (1–6). Hamartin and tuberlin inhibit cell growth through the activity of a complex system of GAP (GTPase-activating protein), specifically the Rheb (Ras homologue enriched in brain) protein, which is dephosphorylated into its GDP-form, and which ultimately inhibits mTORC1 (mammalian/mechanistic target of rapamycin complex 1) (Figures 2A,B). In physiological conditions, mTORC1 activation promotes cell growth, at least in part by increasing the anabolic process of protein synthesis through activation of S6K and inhibition of 4E-BP (3).

Other effects may be due to reduced inhibition of the RHOA and Rac1 pathways, which are essential in cell growth and survival, mesenchymal cell movements, and migration and metastasis of cells, as well as in cell junctions and adhesion maintenance. Additional effects on angiogenesis and cell barrier integrity have also been reported (7–9, 15–17).

TABLE 2 In silico prediction of the effects of protein changes at position 204 of hamartin. The first model evaluates the affinity of the mutated hamartin (inhibitor) to RAC1 (protein); the second reports on the effects on the interactions of hamartin and tuberlin; the third model is taken from *mutationtaster* and evaluates the effects of the substitution of the new amino acid in comparison to the original protein (score 0–150) [see text for explanation].

Protein change	Gene mutation	Phenotype	Effects on Hamartin-Rac1 Interaction		Effects on Hamartin-Tuberlin Interaction		Effect on Hamartin Function
			Predicted $\Delta\Delta G$	Affinity	Enzyme complex with non-inhibitor	Amino acid score (Mutation taster)	
R204P	c.611G > C	TSC	4.49	Decreased	Predicted $\Delta\Delta G$	Affinity	
R204C	c.610C > T	TSC1/FCD	2.03	Decreased	-0.21	Slightly increased	103
R204H	c.611G > A	Present patient	0.54	Slightly decreased	-0.04	Slightly increased	29

TSC, Tuberous sclerosis complex; FCD, Focal cortical dysplasia. $\Delta\Delta G$, binding free energy change (Kcal/mol).

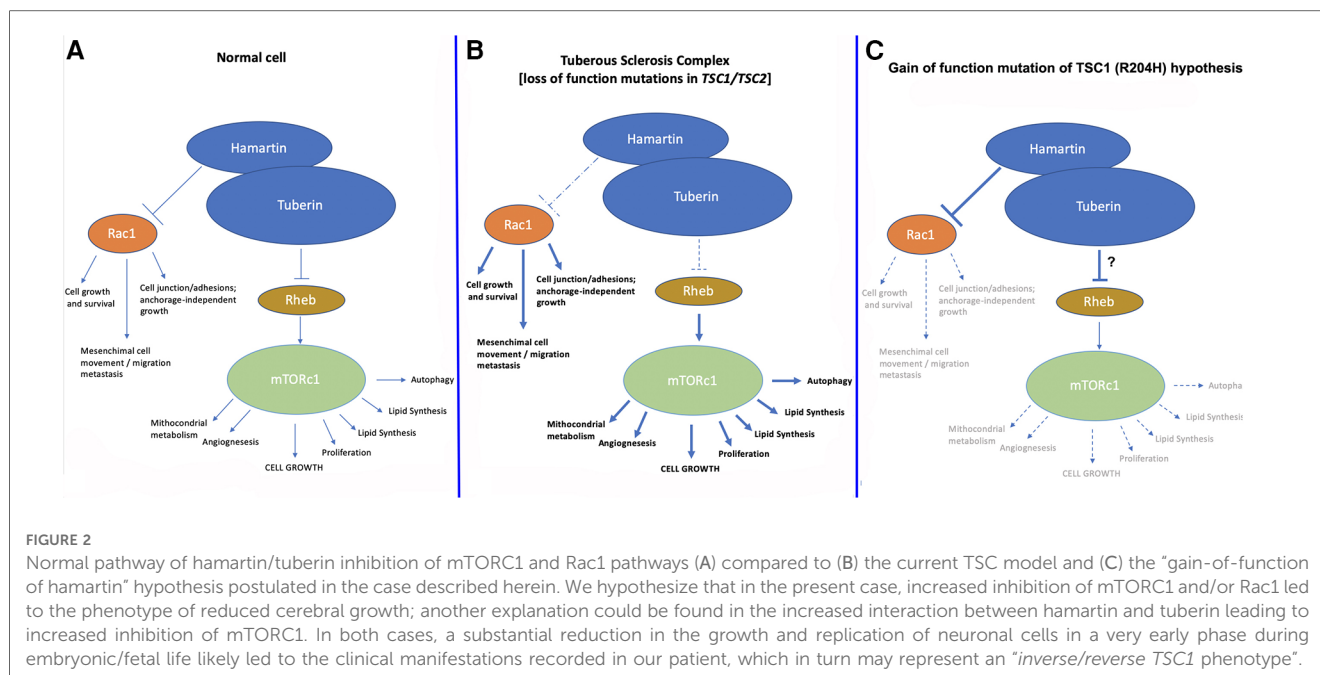


FIGURE 2

Normal pathway of hamartin/tuberin inhibition of mTORC1 and Rac1 pathways (A) compared to (B) the current TSC model and (C) the “gain-of-function of hamartin” hypothesis postulated in the case described herein. We hypothesize that in the present case, increased inhibition of mTORC1 and/or Rac1 led to the phenotype of reduced cerebral growth; another explanation could be found in the increased interaction between hamartin and tuberlin leading to increased inhibition of mTORC1. In both cases, a substantial reduction in the growth and replication of neuronal cells in a very early phase during embryonic/fetal life likely led to the clinical manifestations recorded in our patient, which in turn may represent an “inverse/reverse TSC1 phenotype”.

In our patient, who harbored a novel *TSC1* variant, the phenotype was not compatible with classical TSC, even considering the wide variability of the clinical spectrum of the disease (1). VarCards aggregator of *in-silico* models showed that the mutation/variant recorded herein and occurring within domain 204 of hamartin was a disease-causing one. The site [amino acid 204, exon 8] was within the binding site of tuberlin to Rho proteins; this domain extends from amino acid 145 to 510 and contains the tuberlin-binding site [aa. 302–430]. The closest upstream phosphorylation site is at position 357 and is regulated by kinase GSK3 β .

Given the fact that *in-silico* prediction models “roughly” analyze the protein sequence and report if a missense mutation may give rise to a different protein, but are “unable” to properly analyze a possible “gain-of-function”, we compared the mutation/amino acid substitution R204H to two other “known” variants/substitutions (i.e., R204P and R204C), occurring within the same amino acid and causing classical TSC, to the binding properties of the “mutated” hamartin with Rac1 and tuberlin proteins. Comparison and analysis of these three models provided intriguing results in that all three models showed decreased hamartin affinity to Rac1. Notably, this decrease in affinity, in terms of $\Delta\Delta G$, was very strong for R204P and R204C but milder for R204H (0.54); the affinity with tuberlin (the binding domain of which is very close to the mutated region recorded herein, at position 302–430) showed different results, with some increase in affinity for R204P and R204H (-0.21 and -0.04, respectively) and a decrease for R204C (1.39). The “milder” changes in R204H affinity could be attributed to the “properties” of the two “substituted” amino acids (the original arginine with histidine), which both have basic lateral chains and similar biochemical properties, including a comparable hydrophobic index (-3.2 His, -4.5 Arg), and similar molecular weights (155.1 Da His, 174.2 Da Arg).

The (mildly) decreased affinity to Rac1 could be balanced by the increased binding properties of hamartin to tuberlin, which would therefore strengthen the action of the complex “against” the mTOR activation cascade. As a consequence, the variant hereby recorded would not have the “classical” reduction in function seen in the TSC1/TSC2 dimer complex, although it could have increased the effects on mTOR inhibition and secondarily the Rac1 pathway.

To further confirm the mild effects in terms of loss-of-function of the selected protein, the amino acid score calculated by Mutation Taster gave a “mild” result of 29 (range 0–215), compared to the higher results of the two other mutations/amino acid substitutions (i.e., R204P 103 and R204C 180). In this setting, R204H could be interpreted as a “non-severe” variant that could have some gain-of-function effects on the hamartin-tuberlin complex, thus justifying the clinical phenotype seen in our patient, which comprised primary microcephaly (a malformation with reduced cellular growth/increased apoptosis), simplified gyration, and stunted overall growth (weight and height). In this patient, microcephaly can be regarded as “primary” given its prenatal recording and its manifestations at birth and during follow-up, as well as the association with a pattern of simplified gyration and sulci, in particular in the parietal and occipital regions (Figure 1). Microcephaly does not seem to be acquired, as the mother did not report the use of any drug or substances causing microcephaly *in utero*, nor was there evidence of any congenital infection during pregnancy (18).

The effects of increased inhibition on the mTOR pathway, including microcephaly, have been reported in animal models. In mice, Zhang and colleagues (19) found that inactivation of mTORC1 signaling in postnatal neurons induced reactive astrocyte gliosis. They studied knock-out mice for mTORC1 complex and found that inactivation of mTORC1 in neuronal

progenitors impaired the growth and proliferation of neurons and astrocytes, resulting in a smaller brain and death shortly after birth. In another animal model (20), a transgenic mouse expressing a gain-of-function mutant of mTOR in the forebrain selectively hyperactivated mTORC1 during the embryonic stages with subsequent cortical atrophy, causing prominent apoptosis of neuronal progenitors, associated with upregulation of HIF-1 α ; curiously, and unlike the study by Zhang and colleagues, in postnatal and adult stages, the same hyperactivation resulted in a TSC-similar phenotype with cortical hypertrophy and severe seizures.

In humans, two different phenotypes of brain-reduced growth have been linked to RhoA and Rac1 GTPase, which are critically modulated by hamartin and tuberlin (21). These proteins are members of the Ras superfamily of low molecular weight, monomeric G- proteins: in particular the RhoA, Rac1, and Cdc42 proteins are key regulators of actin cytoskeletal dynamics, and modulate other important cell functions including membrane trafficking, cell cycle progression, gene transcription, adhesion, migration, and survival. A new mosaic neuroectodermal dysplasia syndrome caused by inactivation of the RHOA pathway (which is strictly linked to hamartin inhibition) has been reported [EDFAOB, MIM # 618727], presenting with ectodermal dysplasia in the form of linear hypopigmentation along the lines of Blaschko and alopecia, facial dysmorphisms (e.g., microstomia, malar hypoplasia, down-slanting palpebral fissures and broad nasal bridge), acral (e.g., brachydactyly, syndactyly, broad great toe), ocular (e.g., microphthalmia, myopia, strabismus), dental (e.g., oligodontia, microdontia, conical teeth, abnormal enamel), and brain anomalies including apparently asymptomatic diffuse cortical leukoencephalopathy with ventricular enlargement (10, 15). Individuals with mutations occurring in genes involved in the Rac1 pathway (*RAC1*, *TRIO*) (7–9, 18) have been found to show distinct phenotypes, which include intellectual disability and significant variation of head circumference size; in particular, hypo-activating mutations/variants of Rac1 have been linked to severe microcephaly, while constitutively active substitutions caused macrocephaly. These findings demonstrate that Rac1 is strongly linked to cerebral size (9). Interestingly, mutations in the *TRIO* gene (whose protein product modulates the Rac1 pathway) have similar effects on brain size: macrocephaly or microcephaly depending on the residual functionality of the protein (7, 8).

We hypothesize that the herein-presented *TSCI* variant may have acted as a gain-of-function model of inhibition of the Rho-GTPase-Rac1 pathway (Figure 2C), leading to a somewhat “inverse *TSCI*-hamartin” phenotype. Other explanations could be increased interaction between hamartin and tuberlin leading to increased inhibition of mTORC1 with the substantial reduction of growth and replication of neuronal cells in a very early phase during embryonic/fetal life.

The present study has some limitations: a more powerful tool to prove or disprove pathogenicity would involve the creation of mouse/rat models harboring the same variant and recapitulating

the phenotype; on the other hand, in-silico models like those used for the present study are becoming more practical, easy, and rapid ways to predict the function of a mutated protein.

Moreover, the quality of the imaging protocol (in particular and coronal T1 3D scan and its reformatted images, Figures 1E, F) is low and no longitudinal imaging evaluation nor advanced imaging techniques that better evaluate the CC have been performed so far in the patient.

Data availability statement

The datasets presented in this article are not readily available because of ethical and privacy restrictions. Requests to access the datasets should be directed to the corresponding authors.

Ethics statement

The studies involving human participants were reviewed and approved by Comitato Etico Azienda Ospedaliero Universitaria “Policlinico-San Marco” – Catania, Italy. Written informed consent to participate in this study was provided by the participants’ legal guardian/next of kin. Written informed consent was obtained from the individual(s), and minor(s)’ legal guardian/next of kin, for the publication of any potentially identifiable images or data included in this article.

Author contributions

Conceptualization: ADP, MR, and RF; Methodology: ADP, MR, and RF; Investigation: ADP, MC, AP, and GB; Writing—original draft: ADP, AP, and MR; Writing—review and editing: MR. All authors contributed to the article and approved the submitted version.

Conflict of interest

The authors declare that the research was conducted in the absence of any commercial or financial relationships that could be construed as a potential conflict of interest.

Publisher’s note

All claims expressed in this article are solely those of the authors and do not necessarily represent those of their affiliated organizations, or those of the publisher, the editors and the reviewers. Any product that may be evaluated in this article, or claim that may be made by its manufacturer, is not guaranteed or endorsed by the publisher.

References

- Northrup H, Aronow ME, Bebin EM, Bissler J, Darling TN, de Vries PJ, et al. International Tuberous Sclerosis Complex Consensus Group. Updated international tuberous sclerosis complex diagnostic criteria and surveillance and management recommendations. *Pediatr Neurol.* (2021) 123:50–66. doi: 10.1016/j.pediatrneurol.2021.07.011
- Ruggieri M, Praticò AD. Mosaic neurocutaneous disorders and their causes. *Semin Pediatr Neurol.* (2015) 22:207–33. doi: 10.1016/j.spen.2015.11.001
- Zöllner JP, Franz DN, Hertzberg C, Nabbout R, Rosenow F, Sauter M, et al. A systematic review on the burden of illness in individuals with tuberous sclerosis complex (TSC). *Orphanet J Rare Dis.* (2020) 15:23. doi: 10.1186/s13023-019-1258-3
- Afshar Saber W, Sahin M. Recent advances in human stem cell-based modeling of tuberous sclerosis Complex. *Mol Autism.* (2020) 11:16. doi: 10.1186/s13229-020-0320-2
- Huang J, Manning BD. The TSC1-TSC2 complex: a molecular switchboard controlling cell growth. *Biochem J.* (2008) 412:179–90. doi: 10.1042/BJ20080281
- Reyna-Fabián ME, Hernández-Martínez NL, Alcántara-Ortigoza MA, Ayala-Summano J, Enriquez-Flores S, Velazquez-Aragon JA, et al. First comprehensive TSC1/TSC2 mutational analysis in Mexican patients with tuberous sclerosis Complex reveals numerous novel pathogenic variants. *Sci Rep.* (2020) 10:6589. doi: 10.1038/s41598-020-62759-5
- Barbosa S, Greville-Heygate S, Bonnet M, Godwin A, Fagotto-Kauffman C, Kajava AV, et al. Opposite modulation of RAC1 by mutations in TRIO is associated with distinct, domain-specific neurodevelopmental disorders. *Am J Hum Genet.* (2020) 106:338–55. doi: 10.1016/j.ajhg.2020.01.018
- Pengelly RJ, Greville-Heygate S, Schmidt S, Seaby EG, Reza Jabalameli M, Mehta SG, et al. Mutations specific to the rac-GEF domain of TRIO cause intellectual disability and microcephaly. *J Med Genet.* (2016) 53:735–42. doi: 10.1136/jmedgenet-2016-103942
- Reijnders MRF, Anzor NM, Kousi M, Yue WW, Tan PL, Clarkson K, et al. RAC1 Missense mutations in developmental disorders with diverse phenotypes. *Am J Hum Genet.* (2017) 101:466–77. doi: 10.1016/j.ajhg.2017.08.007
- Ruggieri M, Polizzi A, Catanzaro S, Lo Bianco M, Praticò AD, Di Rocco C. Introduction to phacomatoses (neurocutaneous disorders) in childhood. *Child Nerv Syst.* (2020) 36:2229–68. doi: 10.1007/s00381-020-04758-5
- Geng C, Vangone A, Folkers GE, Xue LC, Bonvin AMJJ. iSEE: interface structure, evolution, and energy-based machine learning predictor of binding affinity changes upon mutations. *Proteins.* (2019) 87:110–9. doi: 10.1002/prot.25630
- Grantham R. Amino acid difference formula to help explain protein evolution. *Science.* (1974) 185:862–4. doi: 10.1126/science.185.4154.862
- Jankauskaite J, Jiménez-García B, Dapkunas J, Fernández-Recio J, Moal IH. SKEMPI 2.0: an updated benchmark of changes in protein-protein binding energy, kinetics and thermodynamics upon mutation. *Bioinformatics.* (2019) 35:462–9. doi: 10.1093/bioinformatics/bty635
- Johansson LF, van Dijk F, de Boer EN, van Dijk-Bos KK, Jongbloed JDH, van der Hout AH, et al. CoNVaDING: single exon variation detection in targeted NGS data. *Hum Mutat.* (2016) 37:457–64. doi: 10.1002/humu.22969
- Vabres P, Sorlin A, Kholmanskikh SS, Demeer B, St-Onge J, Duffourd Y, et al. Postzygotic inactivating mutations of RHOA cause a mosaic neuroectodermal syndrome [published correction appears in nat genet. 2019 nov;51(11):1660] [published correction appears in nat genet. 2020 mar;52(3):353]. *Nat Genet.* (2019) 51:1438–41. doi: 10.1038/s41588-019-0498-4
- Goncharova E, Goncharov D, Noonan D, Krymskaya VP. TSC2 Modulates actin cytoskeleton and focal adhesion through TSC1-binding domain and the Rac1 GTPase. *J Cell Biol.* (2004) 167:1171–82. doi: 10.1083/jcb.200405130
- Ohsawa M, Kobayashi T, Okura H, Igarashi T, Mizuguchi M, Hino O. TSC1 Controls distribution of actin fibers through its effect on function of rho family of small GTPases and regulates cell migration and polarity. *PLoS One.* (2013) 8:e54503. doi: 10.1371/journal.pone.0054503
- Severino M, Geraldo AF, Utz N, Tortora D, Pogledic I, Klonowski W, et al. Definitions and classification of malformations of cortical development: practical guidelines. *Brain.* (2020) 143:2874–94. Erratum in: *Brain* (2020). 143,108. doi: 10.1093/brain/awaa174
- Zhang Y, Xu S, Liang KY, Li K, Zou ZP, Yang CI, et al. Neuronal mTORC1 is required for maintaining the nonreactive state of astrocytes. *J Biol Chem.* (2017) 292:100–11. doi: 10.1074/jbc.M116.744482
- Kassai H, Sugaya Y, Noda S, Nakao K, Maeda T, Kano M, et al. Selective activation of mTORC1 signaling recapitulates microcephaly, tuberous sclerosis, and neurodegenerative diseases. *Cell Rep.* (2014) 7:1626–39. doi: 10.1016/j.celrep.2014.04.048
- Kobayashi K, Sato K, Kida T, Omori K, Hori M, Ozaki H, et al. Stromal cell-derived factor-1 α /C-X-C chemokine receptor type 4 axis promotes endothelial cell barrier integrity via phosphoinositide 3-kinase and Rac1 activation. *Arterioscler Thromb Vasc Biol.* (2014) 34:1716–22. doi: 10.1161/ATVBAHA.114.303890